

Article

# A New Homo-Hexamer Mn-Containing Catalase from *Geobacillus* sp. WCH70

Hai-Chao Li <sup>1</sup>, Qing Yu <sup>1</sup>, Hui Wang <sup>1</sup>, Xin-Yu Cao <sup>1</sup>, Li Ma <sup>1,2,\*</sup> and Zheng-Qiang Li <sup>1,\*</sup>

<sup>1</sup> Key Laboratory for Molecular Enzymology & Engineering, the Ministry of Education, School of Life Sciences, Jilin University, 2699 Qianjin Street, Changchun 130012, Jilin, China; lhc14@mails.jlu.edu.cn (H.-C.L.); 15043113677@163.com (Q.Y.); huiwang15@mails.jlu.edu.cn (H.W.); 18346661052@163.com (X.-Y.C.)

<sup>2</sup> Department of Physics, Georgia Southern University, Statesboro, GA 30460, USA

\* Correspondence: lma@georgiasouthern.edu (L.M.); lzq@jlu.edu.cn (Z.-Q.L.);  
Tel.: +86-0431-85155201 (Z.-Q.L.)

Received: 2 August 2017; Accepted: 12 September 2017; Published: 18 September 2017

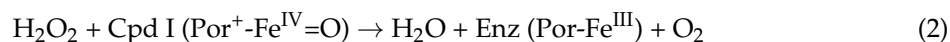
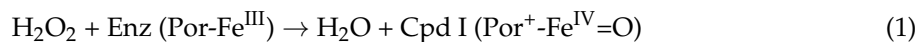
**Abstract:** Catalase is an effective biocatalyst to degrade hydrogen peroxide to water and oxygen that can serve in textile effluent treatment to remove residual H<sub>2</sub>O<sub>2</sub>. Thermostable catalases are needed to withstand both the high temperature and pH of textile wastewater. We have cloned the Mn-containing catalase gene ACS24898.1 from *Geobacillus* sp. WCH70, which originated from thermophilic organisms, and expressed it in *Escherichia coli* in activated form. The recombinant protein has been purified to homogeneity and identified to be a new homo-hexamer Mn-containing catalase. The native molecular mass of the catalase has been measured to be 138 kDa by size-exclusion chromatography. The new enzyme has optimum catalyzed activity at pH 9.0 and a temperature of 75 °C. It is thermostable up to 70 °C for 8 h incubation and maintains 80% and 50% activity, respectively, at 80 °C after 5 h and 90 °C after 1 h. At 75 °C and pH 9.0, the  $K_m$  is 67.26 mM for substrate H<sub>2</sub>O<sub>2</sub> and the rate of reaction at H<sub>2</sub>O<sub>2</sub> saturation,  $V_{max}$ , is 75,300 U/mg. The thermophilic and alkaline preferred properties of this new Mn-catalase are valuable features in textile wastewater treatment.

**Keywords:** Mn-containing catalase; homo-hexamer; *Geobacillus* sp. WCH70; alkaline; thermophilic; textile wastewater

## 1. Introduction

Enzyme catalase (EC 1.11.1.6) mostly exists in aerobic living organisms. Its main function is to catalytically decompose hydrogen peroxide (H<sub>2</sub>O<sub>2</sub>) to water and oxygen in order to protect the cells from oxidative challenging by over-produced H<sub>2</sub>O<sub>2</sub> [1,2]. Catalases also have potential to be industrial enzymes in environmental protection for removing H<sub>2</sub>O<sub>2</sub> containing effluents [3,4]. H<sub>2</sub>O<sub>2</sub> is commonly used as a powerful oxidant in the paper, food, and textile industries [5]. In the textile industry, H<sub>2</sub>O<sub>2</sub> is widely used for bleaching. It is essential to remove the residual H<sub>2</sub>O<sub>2</sub> from industrial waste after the reactions. Traditionally, the removal of residual H<sub>2</sub>O<sub>2</sub> can be done by extensive washing (100 L of water/1 kg of textiles) or using chemicals in the textile industry, which could cause further downstream problems [6]. Tzanov et al. first investigated dyeing in catalase-treated bleaching baths [7]. Catalase could be an effective biocatalyst to degrade H<sub>2</sub>O<sub>2</sub> compared with chemical catalysts [8]. However, common catalases are favorably active at moderate temperatures below 50 °C and at neutral pHs, which limits their application in harsh conditions. For example, in the textile bleaching industry, the wastewater temperature could be more than 60 °C [9]. There is need for thermostable catalases as industrial enzymes in the application of removing H<sub>2</sub>O<sub>2</sub> from waste. One of the approaches will be to discover thermostable catalases from natural sources and to express them in expressing host cells.

Typically catalases are classified as monofunctional heme-containing, bifunctional heme-containing peroxidases-like, and non-heme Mn-containing catalases [10,11]. Heme-containing catalases are widely spread in eukaryotes, bacteria, archaeobacteria, and fungi [10,12]. The reaction of heme-containing catalase to degrade  $\text{H}_2\text{O}_2$  is as follows [13]:



Few monofunctional catalases and bifunctional catalase-peroxidases have been reported to be thermostable so far [14–17]. Therefore, most heme-containing catalases are thermolabile proteins. The active center in a heme catalase is a mononuclear iron porphyrin, regardless of whether it is a mono- or bifunctional one. Unlike heme-containing catalases, Mn-containing catalases have a binuclear manganese complex in a catalytic active center to involve a two-electron oxidation-reduction cycle during turnover. The oxidation state of the dimanganese cluster is transformed between the  $\text{Mn}^{\text{II}}\text{-Mn}^{\text{II}}$  and  $\text{Mn}^{\text{III}}\text{-Mn}^{\text{III}}$  when reacting with  $\text{H}_2\text{O}_2$ . The  $\text{H}_2\text{O}_2$  serves as an oxidant when a  $\text{Mn}^{\text{II}}\text{-Mn}^{\text{II}}$  state exists (Equation (3)), and the  $\text{H}_2\text{O}_2$  serves as a reductant when a  $\text{Mn}^{\text{III}}\text{-Mn}^{\text{III}}$  state exists (Equation (4)) [10].



Until now, all Mn-containing catalases have existed in prokaryotes and archaea [18]. The class of Mn-containing catalases has several features that distinguish it from the class of heme-containing catalases. First, its four-helix bundle protein architecture makes Mn-catalase robust and stable at elevated temperatures [18]. Second, the catalase is relatively sensitive to low  $\text{H}_2\text{O}_2$  concentrations because its intermediate reaction is more stable than that in heme-containing catalases during turnover [18]. Third, Mn-catalase is not sensitive to cyanide inhibition of activity [18].

More than one hundred manganese catalase genes have been submitted to GenBank so far [18]. However, there are only seven Mn-containing catalases that have been purified and characterized. These enzyme genes come from either thermophilic bacteria or archaea. They are *Lactobacillus plantarum* (LPC) [19], *Thermus thermophiles* (TTC) [20], *Thermus* sp. YS 8-13 [21], *Thermoleophilum album* [22], *Pyrobaculum caldifontis* VA1 [23], *Anabaena* PCC7120 (KatB) [24], and *Thermomicrobium roseum* [25]. Purification of the Mn-containing catalases is difficult because the expression level of wild-type catalase is very low. Hence people often clone the target gene into other host cells; for example, *Escherichia coli* [16], *Bacillus subtilis* [26], *Pichia pastoris* [27], *Hansenula polymorpha* [28], and *Lactococcus lactis* [29]. *Escherichia coli* is the most popular host strain for the mature cloning and expression system in which the enzyme can be reproduced quickly and operated easily, but not all the thermophilic catalases can be expressed in activated soluble form [30].

In the present work, we have successfully cloned ACS24898.1, a Mn-containing catalase gene, from *Geobacillus* sp. WCH70 and expressed it in *Escherichia coli* in activated form. *Geobacillus* sp. WCH70 is a novel thermophilic, rod-shaped, Gram-positive facultative anaerobe, for which the optimum growth temperature is 70 °C and the maximum growth temperature is 80 °C [31]. The purified recombinant protein has been proved to be a new homo-hexamer manganese catalase. We name the new catalase GWC (*Geobacillus* sp. WCH70 catalase). Our results show that GWC is thermostable and has optimal activity at pH 9.0 and a temperature of 75 °C. Finally, the kinetic parameters of  $K_m$  and  $V_{\text{max}}$  of this new catalase are reported.

## 2. Results

### 2.1. DNA Sequence and Phylogenetic Analysis of ACS24898.1

The total length of gene sequence ACS24898.1 is 570 bp, and the encoded protein contains 189 amino acids from NCBI (National Center for Biotechnology Information) GenBank. The protein sequences of selected manganese catalases from bacterial or archaea are obtained from PeroxiBase. The phylogenetic tree in Figure 1 is from an analysis in MEGA 7.0.25 using the neighbor-joining (NJ) method with 1000 bootstrap replications. The tree indicates the inferred evolutionary relationships among parts of the known Mn-catalase genes. The manganese catalases of *Thermus thermophilus* (TTC) and *Lactobacillus plantarum* (LPC) belong to two deeply rooted clades [18]. Figure 1 shows that the catalase of *Geobacillus* sp. WCH70 (GWC) has a distant relationship with both TTC and LPC. GWC shares its closest phylogenetic relationship with the manganese catalase of *Heliobacterium modesticaldum* (GenBank: ABZ83254.1), which possesses 190 amino acids. Unfortunately, the *Heliobacterium modesticaldum* catalase has not been purified and characterized. Figure 2 shows the comparison of the protein sequence of GWC with TTC, LPC, and *Heliobacterium modesticaldum* catalase. The protein sequence of GWC is most similar to that of *Heliobacterium modesticaldum*, which shares 62% sequence identity. However, GWC shares 34% and 25% identity with LPC and TTC, respectively. The ion binding amino acids of ACS24898.1 are Glu35, Glu64, His67, Glu135, and His168, which are as conservative as the other three manganese catalase sequences.

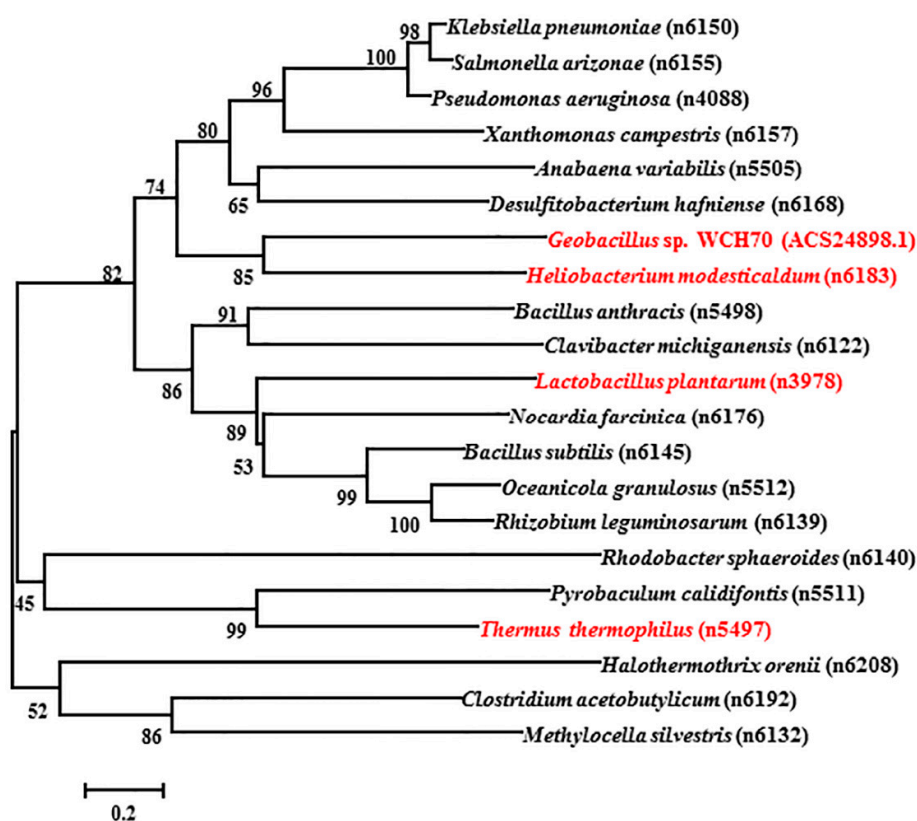


**Figure 1.** Phylogenetic tree of the species of new GWC (*Geobacillus* sp. WCH70 catalase) and 20 related Mn-catalases. The tree is constructed by the neighbor-joining method based on the amino acid sequences of the catalases obtained from PeroxiBase. The test of inferred phylogeny is a bootstrap for 1000 replications. Catalases from *Geobacillus* sp. WCH70 (ACS24898.1), *Heliobacterium modesticaldum* (n6183), *Lactobacillus plantarum* (n3978), and *Thermus thermophilus* (n5497) are marked in red. The relationships between GWC and the species for other three Mn-catalases range from close to far as n6183 > n3978 > n5497.

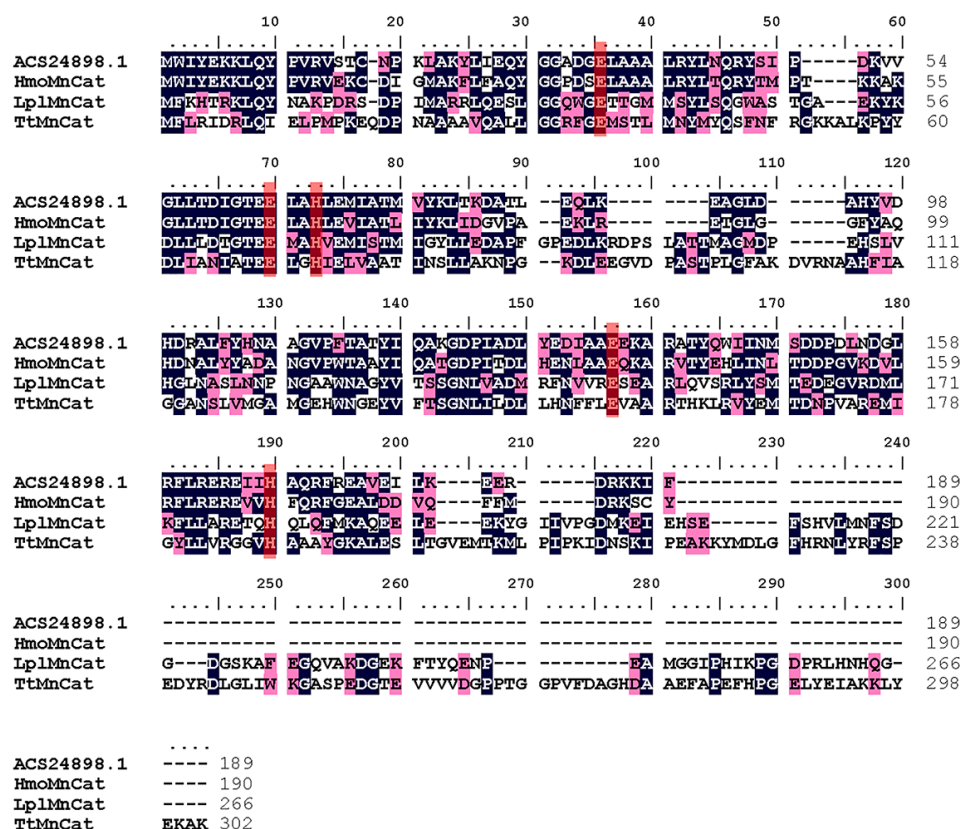


**Figure 2.** Multiple protein sequence alignment of Mn-catalase from *Geobacillus* sp. WCH70 (GWC) and three other Mn-catalases from the PeroxiBase. These sequences are HmoMnCat from *Heliobacterium modesticaldum*, LplMnCat from *Lactobacillus plantarum* (LPC), and TtMnCat from *Thermus thermophilus* (TTC). Identical amino acid residuals are shaded in black, and similar amino acid residuals are shaded in pink. The dimanganese clusters binding amino acids are marked with red. The multiple protein sequence alignments of GWC and three other Mn-catalases from the PeroxiBase are conducted using BioEdit 4.7.2.1.

## 2.2. Gene Cloning Expression and Purification of Recombinant Enzyme

The recombinant plasmid pET20b-MnCAT is shown in Figure S1. The size of the vector is 4178 bp. An Mn-catalase gene (588 bp) with six His tags is inserted close to the T7 promoter. After it was transformed into *E. coli* BL21 (DE3) pLysS cells and induced with isopropyl  $\beta$ -D-1-thiogalactoside (IPTG), the recombinant protein can be expressed mainly in highly soluble form with a large amount of inclusion body. As described in the Section 4.3, there are three purification steps involving multiple heat treatments and an Ni-NTA ( $\text{Ni}^{2+}$  and tris(carboxymethyl) amine) Agarose column chromatograph. The purification processes are monitored by measuring the enzyme activity in combination with sodium dodecyl sulfate polyacrylamide gel electrophoresis (SDS-PAGE) in each step. The results are shown in Table 1 and Figure S2, respectively. If the activity of the crude extract is defined as 1, the activity is doubled after the first heat treatment. Correspondingly, the SDS-PAGE in Figure S2 lane 2 shows that a band between 29.0 and 20.1 kDa is more pronounced (after the first heat treatment) than that in lane 1 (before the heat treatment). The activity further increases 17 fold after the Ni-NTA column, and the purity is greatly improved as shown in Figure S2 lane 3. Finally, after the second heat treatment, a single band appears in lane 4, indicating the homogeneity of the final enzyme. The specific activity of the final enzyme can reach 15,150 U/mg when tested at 60 °C and pH 8.0. It has been observed that the addition of  $\text{Mn}^{2+}$  in the LB (lysogeny broth) medium can substantially increase the targeted enzyme yield (data not shown). This observation agrees that the addition of  $\text{Mn}^{2+}$  helps the catalase to fold properly in *E. coli* cells by incorporating the ions into the active centers of

manganese catalase [25]. The SDS-PAGE can also be used to determine the subunit molecular value. After considering the nonlinear distribution of the molecular mass in SDS-PAGE, we estimate that it is 25 kDa. However, the predicted molecular mass of the nature enzyme with a six His tags is 22.6 kDa according to the amino acid sequence.

**Table 1.** Purification of recombinant enzyme from *E. coli* BL21 (DE3) pLysS.

Method	Total Activity (U)	Total Protein (mg)	Sp Act (Specific Activity) (U/mg)	Yield (%)	Purification (fold)
Crude extract	116,800	317	368	100	1
Heat treatment 1	87,200	128	681	75	2
Ni-NTA (Ni <sup>2+</sup> and tris (carboxymethyl))	62,700	10	6270	54	17
Heat treatment 2	60,600	4	15,150	52	41

### 2.3. Manganese Catalase Identification

Several manganese catalases have been reported to have a homo-hexamer structure such as LPC, TTC, and KatB [24]. In this study, we first determine the subunit molecular mass from SDS-PAGE. As shown in Figure S2 (lane 4), the molecular mass of the subunit is estimated to be 25 kDa. However, the predicted molecular mass of the subunit with a six His tags is 22.6 kDa based on the amino acid sequence. The six His tags might contribute the increase in the molecular mass of the recombinant protein in the SDS result [32]. Next, we determine the native molecular mass from Gel permeation chromatography/size exclusion chromatography GPC/SEC. A standard curve is constructed from four proteins with known molecular masses. As shown in Figure S3, the molecular mass of the purified catalase is calculated to be 138 kDa (solid dot) on the curve. Therefore, the purified enzyme has six subunits per molecule, indicating that GWC is a homo-hexamer in structure. The result from inductively coupled plasma mass spectrometry (ICP-MS) shows that the purified enzyme contains  $1.42 \pm 0.08$  manganese ions per subunit. To further confirm that GWC is a Mn-containing catalase, the response of GWC to cyanide has been tested. Unlike heme-containing catalases, Mn catalase is not sensitive to cyanide [18]. We have examined the residual activities of heme catalase from bovine liver and GWC in the presence of sodium cyanide. The heme catalase retains only 50% of its residual activity after 1  $\mu$ M cyanide treatment. In contrast, there is no observable decrease in the activity of GWC upon the treatment of 100  $\mu$ M cyanide. The insensitive response to cyanide inhibition is further evidence to verify that the new enzyme is a Mn-containing catalase. In addition, the new enzyme has no porphyrin Soret adsorption band (around 400 nm), even when the concentration as high as 1 mg/mL. The results clearly indicate that the purified enzyme GWC is a manganese catalase.

### 2.4. Characteristics of Purified Recombinant Catalase GWC

#### 2.4.1. pH Effect on Catalase Activity

Figure 3a shows the enzyme activity as a function of pH at 25 °C. The maximum activity at pH 9.0 is defined as 100%. The relative activity is below 60% when the pH below 6.0 and remains around 60% up to pH 11, indicating that a weak alkaline environment is preferred. When pH < 5.0, the relative activity is under 50%.

#### 2.4.2. Temperature Effect and Thermostability Testing

The effect of temperature on the activity of the purified enzyme is shown in Figure 3b. The maximum activity at 75 °C is defined as 100%. The result indicates that the activity of the catalase is below 60% when the temperature lower than 50 °C. There is a 20% activity increase when the temperature increases from 55 °C to 60 °C. The relative activity remains above 80% between 60 °C to 80 °C. At 90 °C, the activity retains above 50%. Figure 3c shows the thermostability test of the



catalase. The maximum activity at 0 h of each temperature is defined as 100%. There is no observable change after incubation for 8 h at 70 °C, and the relative activity was still above 85% after incubation for 8 h at 75 °C. The half-life of the catalase at 80 °C and 85 °C is about 7.5 h and 3 h, respectively. However, there is a significant drop in relative activity at 90 °C. The half-life is about 1 h, and there was no more catalase activity after incubation at 90 °C for 4 h.

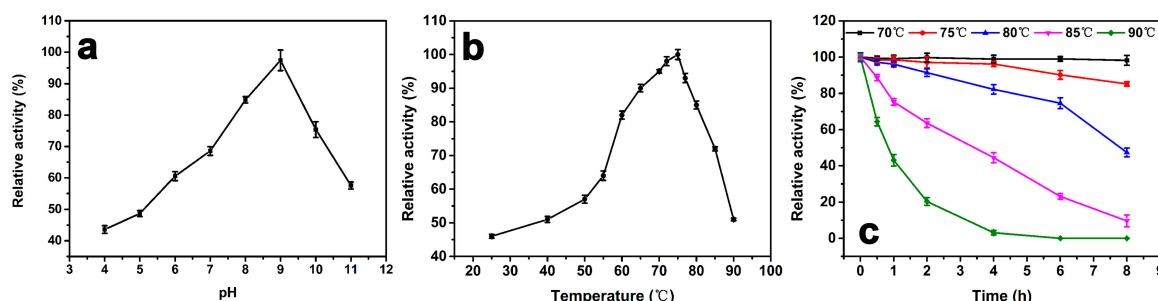


**Figure 3.** (a) The effect of pH on the relative activity of purified GWC. The assays are performed at pHs ranging from 4.0 to 11.0 and a temperature of 25 °C. The maximum activity at pH 9.0 is defined as 100%. (b) The effect of temperature on the relative activity of purified GWC. The assays are at pH 8.0, and the temperatures range from 25 °C to 90 °C. The maximum activity at 75 °C is defined as 100%. (c) Thermostability test of GWC. GWC solutions at 1 µg/mL are pre-incubated at different temperatures ranging from 70 °C to 90 °C at pH 8.0 for 8 h. Then the relative activity of each sample is measured at pH 9.0 and 75 °C. The activity prior to incubation is defined as 100% activity. The data points in the plots are expressed as the mean and standard deviation from three independent measurements.

#### 2.4.3. Kinetic Parameter Determination

The kinetic parameters of the recombinant catalase are determined according to the Lineweaver-Burk plot method with different H<sub>2</sub>O<sub>2</sub> concentrations as substrates. As shown in Figure 4, the linear regression of the plot has a correlation coefficient,  $R^2$ , of 0.9969. The kinetic parameters  $K_m$  and  $V_{max}$  are calculated as 67.26 mM and 75,300 U/mg, respectively.  $K_m$  is an important characteristic of the enzyme, representing its affinity to substrates. The molecular mass of 22.6 kDa per subunit is used to calculate  $k_{cat}$  as  $2.9 \times 10^4 \text{ s}^{-1} \text{ subunit}^{-1}$ .  $k_{cat}/K_m$  is calculated as  $4.22 \times 10^5 \text{ M}^{-1} \cdot \text{s}^{-1}$ .

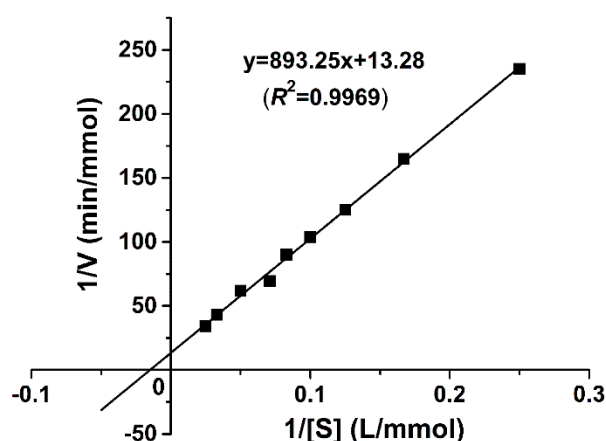


**Figure 4.** Lineweaver-Burk plot of purified GWC kinetics. The  $y$ -axis represents the reciprocal of the reaction rate and the  $x$ -axis is the reciprocal of the substrate concentration. The reactions were carried out at the final fixed GWC concentration of 1 µg/mL and various H<sub>2</sub>O<sub>2</sub> substrate concentrations ranging from 4 to 40 mM at 75 °C with pH 9.0. Each data point is obtained from an average of three independent kinetic measurements. The solid line is the trend-line of the linear regression, with a correlation coefficient of  $R^2 = 0.9969$ .

### 3. Discussion

Normally, a catalase contains a mononuclear heme group in its active sites. Differently, a manganese catalase possesses a binuclear manganese complex in the site without an iron center. The thermostability of GWC is better than most heme catalases due to its four  $\alpha$ -helix bundle robust structure. The half-life of purified GWC is 7.5 h at 80 °C. This result is better than most heme catalases such as those from *Serratia marcescens* SYBC08 (90 min, 60%, 70 °C) [33], *Psychrobacter piscatorii* T-3 (15 min, 50%, 60 °C) [34], *Vibrio salmonicida* (10 min, 0%, 60 °C) [35], *Vibrio rumoiensis* S-1<sup>T</sup> (15 min, 0%, 60 °C) [36], *Halomonas* sp. SK1 (30 min, 0%, 55 °C) [37], *Psychrobacter piscatorii* (15 min, 20%, 65 °C) [38], and *Geobacillus* sp. CHB1 (60 min, 10%, 80 °C) [14]. However, GWC is not as stable as some other Mn-catalases such as *Thermus* sp. YS 8-13 catalase (3 h, 100%, 90 °C) and *P. calidifontis* VA1 catalase (432 min, 50%, 90 °C). The peptide chain of GWC (189 amino acids) is shorter than those of previously reported manganese catalases such as LPC (266 amino acids), TTC (302 amino acids), *Thermus* sp. YS 8-13 catalase (302 amino acids), and *P. calidifontis* VA1 catalase (298 amino acids) from NCBI GenBank. Unlike most manganese catalases, GWC has no C-terminal tail revealed by SWISS-MODEL. Hydrogen bonds and salt bridges are the main forces of its homo-hexamer assembly, and a loss of the C-terminal tail contributes to smaller number of hydrogen bonds and salt bridges [24]. Moreover, the Ca<sup>2+</sup> binding site in the C-terminal tail may stabilize the homo-hexamer structure [24]. Therefore, the homo-hexamer structure of GWC may not be as stable as that of other manganese catalases from *Thermus* sp. YS 8-13 or *P. calidifontis* VA1. We suggest that this is the reason why GWC quickly became inactive above 90 °C. Nevertheless, compared to most heme catalases mentioned above, GWC shows better thermo-stability due to the four  $\alpha$ -helix bundle structure of its subunit [18].

In the present study, the manganese content is  $1.42 \pm 0.08$  ions per subunit of Mn-catalase, as determined by ICP-MS. This value is close to those for other manganese catalases in previous studies such as  $1.12 \pm 0.37$  atoms/subunit (*Lactobacillus plantarum* [19]), 1.2 atoms/subunit (*Thermus* sp. YS 8-13 [21]),  $1.4 \pm 0.4$  atoms/subunit (*Thermoleophilum album* [22]), and  $1.32 \pm 0.03$  atoms/subunit (*Pyrobaculum calidifontis* VA1 [23]). These values are lower than crystal structure data (two manganese atoms/subunit), which could be due to a loss of manganese ions during purification [23]. The native molecular mass is 138 kDa according to GPC/SEC, and the molecular mass of one subunit is 22.6 kDa. Therefore, the catalase is supposed to be a homo-hexamer enzyme like manganese catalases from *Lactobacillus plantarum* [19], *Thermus thermophiles* [20], *Thermus* sp. YS 8-13 [21], and *Anabaena* PCC7120 [24]. Kinetic analysis of GWC shows a  $K_m$  value of 67.26 mM and a  $k_{cat}$  value of  $2.9 \times 10^4 \text{ s}^{-1} \text{ subunit}^{-1}$  toward H<sub>2</sub>O<sub>2</sub>. The kinetic parameters are comparable to the previously reported manganese catalases, as Table 2 shows.

**Table 2.** The kinetic parameters of GWC compared with those of other characterized Mn-catalases.

Mn-Catalase	$k_{cat}$ ( $\text{s}^{-1} \cdot \text{subunit}^{-1}$ )	$K_m$ (mM)	$k_{cat}/K_m$ ( $\text{M}^{-1} \text{ s}^{-1}$ )	Reference
<i>Lactobacillus plantarum</i>	$3.3 \times 10^4$	350	$9.4 \times 10^4$	[19]
<i>Thermus thermophiles</i>	$2.6 \times 10^5$	83	$3.1 \times 10^6$	[20]
<i>Thermoleophilum album</i>	$6.2 \times 10^3$	15	$4.1 \times 10^5$	[22]
<i>Pyrobaculum calidifontis</i>	$2.9 \times 10^4$	170	$1.7 \times 10^5$	[23]
<i>Anabaena</i> PCC7120	$2.23 \times 10^4$	1.63	$1.35 \times 10^7$	[24]
<i>Thermomicrobium roseum</i>	$2.02 \times 10^4$	20	$1.01 \times 10^6$	[25]
<i>Geobacillus</i> sp. WCH70	$2.9 \times 10^4$	67.26	$4.22 \times 10^5$	This work

### 4. Materials and Methods

#### 4.1. Amino Acid Sequences Analysis

We examined the phylogenetic relationships of ACS24898.1 compared with other bacterial or archaea manganese catalases. The protein sequences were obtained from the PeroxiBase. The relationships of the sequences were built using MEGA 7.0.25 (Pennsylvania State University,

State College, PA, USA). The trees were constructed by the neighbor-joining method. The test of inferred phylogeny was bootstrapped for 1000 replications. The multiple protein sequence alignments of GWC and three other Mn-catalases from the PeroxiBase were conducted using BioEdit 4.7.2.1 (Isis Pharmaceuticals, Inc., Carlsbad, CA, USA). These sequences were HmoMnCat from *Heliobacterium modesticaldum*, LplMnCat from *Lactobacillus plantarum* (LPC), and TtMnCat from *Thermus thermophilus* (TTC).

#### 4.2. Expression Vector Construction

The *Geobacillus* sp. WCH70 [31] in freeze-dried form was purchased from the China Center of Industrial Culture Collection (CICC) (Beijing, China). The culture was aerobically grown in 50 mL medium containing 5 g tryptone, 3 g beef extract, and 5 g NaCl (Sinopharm Chemical Reagent Co., Ltd., Beijing, China) per liter at pH 7.5 and 70 °C, with shaking at 180 rpm for 18 h. The genome of *Geobacillus* sp. WCH70 was extracted by a Rapid Bacterial Genomic DNA Isolation Kit (Sangon Biotech, Shanghai, China). It was used as a Polymerase Chain Reaction (PCR) template. The catalase gene from *Geobacillus* sp. WCH70 was amplified by PCR with Ex Taq<sup>®</sup> (TaKaRa, Dalian, China) and primers (forward primer: 5'-GGAATTCATATGTGGATTTATGAAA-AAAAATTGCAATAT-3' and reverse primer: 5'-CCGCTCGAGTTAGTGATGGTGATGGTG-ATGAAAAATTTTCTTGCG-3'). 5'-GGAATTC-3' and 5'-CCG-3' were protective bases. 5'-CATATG-3' and 5'-CTCGAG-3' represented the Nde I and Xho I restriction enzyme cutting sites. We introduced a His-tag sequence (5'-GTGATGGTGATGGTGATG-3') in the reverse primer. The primers were designed using Primer 5.0. The PCR program was set as follows: denaturing (5 min, 95 °C), followed by 30 cycles of denaturing (30 s, 95 °C), annealing (30 s, 55 °C), polymerization (1 min, 72 °C), and final polymerization (10 min, 72 °C). The expression vector pET20b (TaKaRa, Dalian, China) and the PCR product were digested separately with the restriction enzymes Nde I and Xho I (TaKaRa, Dalian, China). The digested product was ligated with T<sub>4</sub> DNA ligase (TaKaRa, Dalian, China) after agarose gel purification. At last, the recombinant plasmid was transformed into *E. coli* BL21 (DE3) pLysS (Novagen, Madison, WI, USA). The catalase sequence was confirmed by Sangon Biotech (Shanghai, China). For seeding cell preparation, the recombinant strains were cultured in 50 mL LB medium (10 g tryptone (Oxoid, UK), 5 g yeast extract (Oxoid, UK) and 10 g NaCl per liter, at pH 7.0) with 50 µg/mL ampicillin and 34 µg/mL chloramphenicol (Sigma, St. Louis, MO, USA).

#### 4.3. Expression and Purification of Recombinant Enzyme

The recombinant strains from above were cultured in 2 L LB medium, with a Mn<sup>2+</sup> concentration of 100 µM, and grown at 37 °C, with shaking at 180 rpm. When OD<sub>600</sub> reached 1.8, a solution of isopropyl β-D-1-thiogalactoside (IPTG) was added into the culture to a final concentration of 0.5 mM. Then the culture continued growing at 28 °C, with shaking at 120 rpm for 16 h. The cells were harvested by centrifugation at 8000× g for 10 min and suspended in Tris-HCl (20 mM, pH 8.0) buffer. The suspended cells were lysed by ultrasonication and centrifuged a second time at 18,000× g for 10 min to remove cell walls. The supernatant was incubated at 60 °C for 30 min then centrifuged again at 18,000× g for 10 min to remove most heat-labile proteins. The new supernatant was loaded on a Ni-NTA Agarose column (Cube Biotech, Monheim am Rhein, Germany). The column was first washed with 20 mM Tris-HCl (pH 8.0) buffer to remove impurities until the absorbance at 280 nm was not detectable by NanoDrop 2000C (Thermo Fisher, Waltham, MA, USA). The column then was eluted with the same buffer but containing 100 mM imidazole. The elution was collected when the absorbance at 280 nm appeared. The collected solution was dialyzed (MW 3000) against 20 mM Tris-HCl (pH 8.0) buffer three times. Finally, the retentate was incubated at 70 °C for 1 h and then centrifuged at 18,000× g for 10 min. The collected supernatant was ready for analysis. The protein purity was determined by 15% SDS-PAGE (BIO-RAD, Hercules, CA, USA) gel electrophoresis [39], and the concentration was measured by Bradford assay using a standard protein curve constructed from eight concentrations of bovine serum albumin (BSA) [40].



#### 4.4. Metal Analysis and Molecular Size Determination

The purified enzyme was diluted to 50  $\mu\text{g}/\text{mL}$  in 20 mM at pH 7.0 in Tris-HCl buffer and analyzed for Mn ions using inductively coupled plasma mass spectrometry (ICP-MS) (HR-ICP-MS, Thermo Fisher, Waltham, MA, USA). The native protein size was determined using a Bio-Gel SEC 40-XL size-exclusion column (Bio-Rad, Hercules, CA, USA),  $300 \times 7.8$  mm, eluted with potassium phosphate buffer (20 mM, pH 7.0) at a flow rate of 0.5 mL/min controlled by a Viscotek 270 GPC/SEC system (Malvern, Malvern, UK). The standard molecular size curve was constructed by conalbumin (75 kDa), aldolase (158 kDa), ferritin (440 kDa), and thyroglobulin (669 kDa). SDS-PAGE was used to determine the molecular mass of the subunit. We also tested sodium cyanide (the final concentration was 100  $\mu\text{M}$  and 1  $\mu\text{M}$ ) for an inhibiting effect on the purified protein and bovine liver (Sigma, St. Louis, MO, USA).

#### 4.5. Enzyme Activity Characterization

The activity of the purified enzyme was tested with substrates and  $\text{H}_2\text{O}_2$ . The activity assay was performed according to Beers Jr. and Sizer [41]. The reaction was monitored at 240 nm ( $\epsilon_{240} = 43.6 \text{ M}^{-1} \text{ cm}^{-1}$ ) of the  $\text{H}_2\text{O}_2$  adsorption peak [42] using a UV-2700 spectrophotometer (Shimadzu, Kyoto, Japan). The purified catalase was diluted to a concentration of about 1  $\mu\text{g}/\text{mL}$  by Tris-HCl (20 mM, pH 8.0) buffer, and the  $\text{H}_2\text{O}_2$  was diluted to 20 mM with various pH buffers. Then 50  $\mu\text{L}$  enzyme solution was mixed with 950  $\mu\text{L}$   $\text{H}_2\text{O}_2$  solution at specified temperatures controlled by a water bath. The reaction was monitored for 1 min. One unit of catalase activity was defined as the amount of enzyme required to convert 1  $\mu\text{mol}$  of  $\text{H}_2\text{O}_2$  to  $\text{H}_2\text{O}$  and  $\text{O}_2$  per min. Each measurement was conducted three times. To study the effect of pH on the activity, the  $\text{H}_2\text{O}_2$  was diluted with citrate buffer (pH 4.0, 5.0, and 6.0), Tris-HCl buffer (pH 7.0, 8.0, and 9.0), or Gly-NaOH buffer (pH 10.0 and 11.0). The reaction was kept at 25  $^\circ\text{C}$ . The optimum temperature assay was performed at pH 8.0 in 20 mM Tris-HCl buffer. The enzyme solution was pre-incubated and kept at different temperatures ranging from 25  $^\circ\text{C}$  to 90  $^\circ\text{C}$ . To assay the enzyme thermostability, 20  $\mu\text{g}/\text{mL}$  diluted enzyme was incubated at 60  $^\circ\text{C}$ , 70  $^\circ\text{C}$ , 80  $^\circ\text{C}$ , 85  $^\circ\text{C}$ , and 90  $^\circ\text{C}$  for 8 h. During the incubation, samples were collected at different time points for the activity assay. Then the relative activity of each sample was measured at 75  $^\circ\text{C}$  at pH of 9.0 in 20 mM Tris-HCl buffer. For a kinetic study, the purified enzyme at a fixed final concentration of 1  $\mu\text{g}/\text{mL}$  reacted with  $\text{H}_2\text{O}_2$  at different concentrations ranging from 4 to 40 mM at 75  $^\circ\text{C}$  and pH 9.0. The reaction was monitored at the  $\text{H}_2\text{O}_2$  characteristic absorption peak of 240 nm for 1 min. The change in the substrate concentrations over time was recorded. Each reaction was duplicated three times. An average reaction velocity (rate) was calculated from each kinetic curve. A Lineweaver-Burk plot (double-reciprocal plot) was constructed using the reciprocal of the rate as the  $y$ -axis and the reciprocal of the substrate concentration as the  $x$ -axis. The kinetic parameter of the maximum reaction velocity,  $V_{\text{max}}$ , was calculated from the inverse of the  $y$ -intercept and  $K_m$ , the substrate concentration at half the reaction rate, from the slope of the plot according to Lineweaver and Burk [43].

## 5. Conclusions

In this paper, we successfully cloned the Mn-catalase gene from *Geobacillus* sp. WCH70 and then expressed it in *E. coli* BL21 (DE3) pLysS cells for the first time. We have purified and characterized the enzyme and identified it as a new thermophilic manganese catalase (GWC). It possesses the smallest subunit (22.6 kDa) compared with the other reported manganese catalases. The maximum specific activity of GWC is 75,300 U/mg at 75  $^\circ\text{C}$  and pH 9.0. The catalase shows high activity over the temperature range from 60 to 80  $^\circ\text{C}$ . In addition, the catalase shows high activity in weak alkaline environments, with a maximum at pH 9.0. The results suggest that this new manganese catalase is promising in the textile, paper-making, and other industries for removing  $\text{H}_2\text{O}_2$ .

**Supplementary Materials:** The following are available online at [www.mdpi.com/2073-4344/7/9/277/s1](http://www.mdpi.com/2073-4344/7/9/277/s1), Figure S1: Recombinant plasmid of pET20b-MnCAT map, Figure S2: Coomassie-blue stained SDS-PAGE gel of the enzyme, and Figure S3: Gel filtration analysis of purified GWC.

**Acknowledgments:** The authors are grateful for the financial support from the National Natural Science Foundation of China (Grant Numbers: 31670797).

**Author Contributions:** Hai-Chao Li and Zheng-Qiang Li conceived and designed the experiments; Qing Yu and Xin-Yu Cao performed the experiments; Hui Wang analyzed the data; Li Ma contributed reagents/materials/analysis tools; and Hai-Chao Li wrote the paper.

**Conflicts of Interest:** The authors declare no conflicts of interest.

## References

1. Oscar, L.; Oscar, C.B. *Physiological Studies of Connecticut Leaf Tobacco*; United States Department of Agriculture: Washington, DC, USA, 1900; Volume 56, pp. 5–57.
2. Qin, J.; Lu, M.-X.; Zheng, Y.-T.; Du, Y.-Z. Molecular cloning, characterization, and functional analysis of catalase in *Frankliniella occidentalis* (Thysanoptera: Thripidae). *Ann. Entomol. Soc. Am.* **2017**, *110*, 212–220.
3. Wang, H.-X.; Tokusige, Y.; Shinoyama, H.; Fujii, T.; Urakami, T. Purification and characterization of a thermostable catalase from culture broth of *Thermoascus aurantiacus*. *J. Ferment. Bioeng.* **1998**, *85*, 169–173. [[CrossRef](#)]
4. Sharif, A.; Ashraf, M.; Javeed, A.; Anjum, A.A.; Akhtar, M.F.; Akhtar, B.; Saleem, A. Oxidative stress responses in Wistar rats on subacute exposure to pharmaceutical wastewater. *Environ. Sci. Pollut. Res.* **2016**, *23*, 24158–24165. [[CrossRef](#)] [[PubMed](#)]
5. Zeng, H.-W.; Cai, Y.-J.; Liao, X.-R.; Qian, S.-L.; Zhang, F.; Zhang, D.-B. Optimization of catalase production and purification and characterization of a novel cold-adapted Cat-2 from mesophilic bacterium *Serratia marcescens* SYBC-01. *Ann. Microbiol.* **2010**, *60*, 701–708. [[CrossRef](#)]
6. Paar, A.; Costa, S.; Tzanov, T.; Gudelj, M.; Robra, K.H.; Cavaco-Paulo, A.; Gübitz, G.M. Thermo-alkali-stable catalases from newly isolated *Bacillus* sp. for the treatment and recycling of textile bleaching effluents. *J. Biotechnol.* **2001**, *89*, 147–153. [[CrossRef](#)]
7. Tzanov, T.; Costa, S.; Guebitz, G.M.; Cavaco-Paulo, A. Dyeing in catalase-treated bleaching baths. *Color. Technol.* **2010**, *117*, 1–5. [[CrossRef](#)]
8. Fu, X.-H.; Wang, W.; Hao, J.-H.; Zhu, X.-L.; Sun, M. Purification and characterization of catalase from marine bacterium *Acinetobacter* sp. YS0810. *BioMed Res. Int.* **2014**, *2014*, 409626. [[CrossRef](#)] [[PubMed](#)]
9. Josef, D.; Wolfgang, S. The mechanism of hydrogen peroxide bleaching. *Text. Chem. Color.* **1996**, *28*, 24–28.
10. Chelikani, P.; Fita, I.; Loewen, P.C. Diversity of structures and properties among catalases. *Cell. Mol. Life Sci.* **2004**, *61*, 192–208. [[CrossRef](#)] [[PubMed](#)]
11. Grigoras, A.G. Catalase immobilization—A review. *Biochem. Eng. J.* **2017**, *117*, 1–20. [[CrossRef](#)]
12. Pradhan, A.; Herrero-de-Dios, C.; Belmonte, R.; Budge, S.; Garcia, A.L.; Kolmogorova, A.; Lee, K.K.; Martin, B.D.; Ribeiro, A.; Bebes, A.; et al. Elevated catalase expression in a fungal pathogen is a double-edged sword of iron. *PLoS Pathog.* **2017**, *13*, e1006405. [[CrossRef](#)] [[PubMed](#)]
13. Switala, J.; Loewen, P.C. Diversity of properties among catalases. *Arch. Biochem. Biophys.* **2002**, *401*, 145–154. [[CrossRef](#)]
14. Jia, X.-B.; Chen, J.-C.; Lin, C.-Q.; Lin, X.-J. Cloning, expression, and characterization of a novel thermophilic monofunctional catalase from *Geobacillus* sp. CHB1. *BioMed Res. Int.* **2016**, *2016*, 7535604. [[CrossRef](#)] [[PubMed](#)]
15. Thompson, V.S.; Schaller, K.D.; Apel, W.A. Purification and characterization of a novel thermo-alkali-stable catalase from *Thermus brockianus*. *Biotechnol. Prog.* **2003**, *19*, 1292–1299. [[CrossRef](#)] [[PubMed](#)]
16. Ebara, S.; Shigemori, Y. Alkali-tolerant high-activity catalase from a thermophilic bacterium and its overexpression in *Escherichia coli*. *Protein Expr. Purif.* **2008**, *57*, 255–260. [[CrossRef](#)] [[PubMed](#)]
17. Yu, Z.-X.; Zheng, H.-C.; Zhao, X.-Y.; Li, S.-F.; Xu, J.-Y.; Song, H. High level extracellular production of a recombinant alkaline catalase in *E. coli* BL21 under ethanol stress and its application in hydrogen peroxide removal after cotton fabrics bleaching. *Bioresour. Technol.* **2016**, *214*, 303–310. [[CrossRef](#)] [[PubMed](#)]
18. Whittaker, J.W. Non-heme manganese catalase—The ‘other’ catalase. *Arch. Biochem. Biophys.* **2011**, *525*, 111–120. [[CrossRef](#)] [[PubMed](#)]

19. Kono, Y.; Fridovich, I. Isolation and characterization of the pseudocatalase of *Lactobacillus plantarum*. *J. Biol. Chem.* **1983**, *258*, 6015–6019. [[PubMed](#)]
20. Barynin, V.V.; Grebenko, A.I. T-catalase is a nonheme catalase of the extremally thermophilic bacterium *Thermus thermophilus* HB8. *Dokl. Akad. Nauk SSSR* **1986**, *286*, 461–464.
21. Kagawa, M.; Murakoshi, N.; Nishikawa, Y.; Matsumoto, G.; Kurata, Y.; Mizobata, T.; Kawata, Y.; Nagai, J. Purification and cloning of a thermostable manganese catalase from a thermophilic bacterium. *Arch. Biochem. Biophys.* **1999**, *362*, 346–355. [[CrossRef](#)] [[PubMed](#)]
22. Allgood, G.S.; Perry, J.J. Characterization of a manganese-containing catalase from the obligate thermophile *Thermoleophilum album*. *J. Bacteriol.* **1986**, *168*, 563–567. [[CrossRef](#)] [[PubMed](#)]
23. Amo, T.; Atomi, H.; Imanaka, T. Unique presence of a manganese catalase in a hyperthermophilic archaeon, *Pyrobaculum calidifontis* VA1. *J. Bacteriol.* **2002**, *184*, 3305–3312. [[CrossRef](#)] [[PubMed](#)]
24. Bihani, S.C.; Chakravarty, D.; Ballal, A. KatB, a cyanobacterial Mn-catalase with unique active site configuration: Implications for enzyme function. *Free Radic. Biol. Med.* **2016**, *93*, 118–129. [[CrossRef](#)] [[PubMed](#)]
25. Baginski, R.; Sommerhalter, M. A manganese catalase from *Thermomicrobium roseum* with peroxidase and catecholase activity. *Extremophiles* **2016**, *21*, 201–210. [[CrossRef](#)] [[PubMed](#)]
26. Shi, X.-L.; Feng, M.-Q.; Zhao, Y.-J.; Guo, X.; Zhou, P. Overexpression, purification and characterization of a recombinant secretory catalase from *Bacillus subtilis*. *Biotechnol. Lett.* **2008**, *30*, 181–186. [[CrossRef](#)] [[PubMed](#)]
27. Shi, X.-L.; Feng, M.-Q.; Shi, J.; Shi, Z.-H.; Zhong, J.; Zhou, P. High-level expression and purification of recombinant human catalase in *Pichia pastoris*. *Protein Expr. Purif.* **2007**, *54*, 24–29. [[CrossRef](#)] [[PubMed](#)]
28. Gellissen, G.; Piontek, M.; Dahlems, U.; Jenzelewski, V.; Gavagan, J.E.; Dicosimo, R.; Anton, D.L.; Janowicz, Z.A. Recombinant *Hansenula polymorpha* as a biocatalyst: Coexpression of the spinach glycolate oxidase (GO) and the *S. cerevisiae* catalase T (CTT1) gene. *Appl. Microbiol. Biotechnol.* **1996**, *46*, 46–54. [[CrossRef](#)] [[PubMed](#)]
29. Rochat, T.; Miyoshi, A.; Gratadoux, J.J.; Duwat, P.; Sourice, S.; Azevedo, V.; Langella, P. High-level resistance to oxidative stress in *Lactococcus lactis* conferred by *Bacillus subtilis* catalase KatE. *Microbiology* **2005**, *151*, 3011–3018. [[CrossRef](#)] [[PubMed](#)]
30. Hidalgo, A.; Betancor, L.; Moreno, R.; Zafra, O.; Cava, F.; Fernández-Lafuente, R.; Guisán, J.M.; Berenguer, J. *Thermus thermophilus* as a cell factory for the production of a thermophilic Mn-dependent catalase which fails to be synthesized in an active form in *Escherichia coli*. *Appl. Environ. Microbiol.* **2004**, *70*, 3839–3844. [[CrossRef](#)] [[PubMed](#)]
31. Brumm, P.J.; Land, M.L.; Mead, D.A. Complete genome sequences of *Geobacillus* sp. WCH70, a thermophilic strain isolated from wood compost. *Stand. Genom. Sci.* **2016**, *11*. [[CrossRef](#)] [[PubMed](#)]
32. Zhong, Y.-B.; Zhang, X.-H.; Chen, J.-X.; Chi, Z.-H.; Sun, B.-G.; Li, Y.; Austin, B. Overexpression, purification, characterization, and pathogenicity of *Vibrio harveyi* hemolysin VHH. *Infect. Immun.* **2006**, *74*, 6001–6005. [[CrossRef](#)] [[PubMed](#)]
33. Zeng, H.-W.; Cai, Y.-J.; Liao, X.-R.; Zhang, F.; Zhang, D.-B. Production, characterization, cloning and sequence analysis of a monofunctional catalase from *Serratia marcescens* SYBC08. *J. Basic Microbiol.* **2011**, *51*, 205–214. [[CrossRef](#)] [[PubMed](#)]
34. Kimoto, H.; Yoshimune, K.; Matsuyama, H.; Yumoto, I. Characterization of catalase from psychrotolerant *Psychrobacter piscatorii* T-3 exhibiting high catalase activity. *Int. J. Mol. Sci.* **2012**, *13*, 1733–1746. [[CrossRef](#)] [[PubMed](#)]
35. Lorentzen, M.S.; Moe, E.; Jouve, H.M.; Willassen, N.P. Cold adapted features of *Vibrio salmonicida* catalase: Characterisation and comparison to the mesophilic counterpart from *Proteus mirabilis*. *Extremophiles* **2006**, *10*, 427–440. [[CrossRef](#)] [[PubMed](#)]
36. Yumoto, I.; Ichihashi, D.; Iwata, H.; Istokovics, A.; Ichise, N.; Matsuyama, H.; Okuyama, H.; Kawasaki, K. Purification and characterization of a catalase from the facultatively psychrophilic bacterium *Vibrio rumoiensis* S-1<sup>T</sup> exhibiting high catalase activity. *J. Bacteriol.* **2000**, *182*, 1903–1909. [[CrossRef](#)] [[PubMed](#)]
37. Phucharoen, K.; Hoshino, K.; Takenaka, Y.; Shinozawa, T. Purification, characterization, and gene sequencing of a catalase from an alkali- and halo-tolerant bacterium, *Halomonas* sp. SK1. *Biosci. Biotechnol. Biochem.* **2002**, *66*, 955–962. [[CrossRef](#)] [[PubMed](#)]
38. Wang, W.; Sun, M.; Liu, W.-S.; Zhang, B. Purification and characterization of a psychrophilic catalase from Antarctic *Bacillus*. *Can. J. Microbiol.* **2008**, *54*, 823–828. [[CrossRef](#)] [[PubMed](#)]

39. Laemmli, U.K. Cleavage of structural proteins during the assembly of the head of bacteriophage T4. *Nature* **1970**, *227*, 680–685. [[CrossRef](#)] [[PubMed](#)]
40. Bradford, M.M. A rapid and sensitive method for the quantitation of microgram quantities of protein utilizing the principle of protein-dye binding. *Anal. Biochem.* **1976**, *72*, 248–254. [[CrossRef](#)]
41. Beers, R.F.; Sizer, I.W. A spectrophotometric method for measuring the breakdown of hydrogen peroxide by catalase. *J. Biol. Chem.* **1952**, *195*, 133–140. [[PubMed](#)]
42. Hildebrandt, A.G.; Roots, I. Reduced nicotinamide adenine dinucleotide phosphate (NADPH)-dependent formation and breakdown of hydrogen peroxide during mixed function oxidation reactions in liver microsomes. *Arch. Biochem. Biophys.* **1975**, *171*, 385–397. [[CrossRef](#)]
43. Lineweaver, H.; Burk, D. The determination of enzyme dissociation constants. *J. Am. Chem. Soc.* **1934**, *56*, 658–666. [[CrossRef](#)]



© 2017 by the authors. Licensee MDPI, Basel, Switzerland. This article is an open access article distributed under the terms and conditions of the Creative Commons Attribution (CC BY) license (<http://creativecommons.org/licenses/by/4.0/>).